nature communications

Article

https://doi.org/10.1038/s41467-024-50685-3

Superiority of native soil core microbiomes in supporting plant growth

Received: 13 December 2023

Accepted: 18 July 2024

Published online: 04 August 2024

Check for updates

Yanyan Zhou[1,6], Donghui Liu[1,6], Fengqiao Li[1], Yuanhua Dong[2], Zhili Jin[3], Yangwenke Liao[1], Xiaohui Li[3], Shuguang Peng[4] ✉, Manuel Delgado-Baquerizo[5] & Xiaogang Li[1] ✉

Native core microbiomes represent a unique opportunity to support food provision and plant-based industries. Yet, these microbiomes are often neglected when developing synthetic communities (SynComs) to support plant health and growth. Here, we study the contribution of native core, native non-core and non-native microorganisms to support plant production. We construct four alternative SynComs based on the excellent growth promoting ability of individual stain and paired non-antagonistic action. One of microbiome based SynCom (SC2) shows a high niche breadth and low average variation degree in-vitro interaction. The promoting-growth effect of SC2 can be transferred to non-sterile environment, attributing to the colonization of native core microorganisms and the improvement of rhizosphere promoting-growth function including nitrogen fixation, IAA production, and dissolved phosphorus. Further, microbial fertilizer based on SC2 and composite carrier (rapeseed cake fertilizer + rice husk carbon) increase the net biomass of plant by 129%. Our results highlight the fundamental importance of native core microorganisms to boost plant production.

The soil microbiome is considered to hold vast potential to support food production and plant-based industries[1–3]. Yet, we are still very far from understanding what microbial taxa can help us to support plant growth. Many of the commercial products are based on easy to culture and non-native microorganisms for the location wherein the product is being applied[4,5]. This application provides an alternative to promote plant health, nutrition, and growth[6,7], through various mechanisms, including the production of indoleacetic acid and siderophore, the fixation of nitrogen, and the dissolution phosphorus[8,9]. However, microorganisms adapted to a particular soil environment usually have difficulties in colonizing new environments and translating their functional capacities to other soils[1,10]. Moreover, inoculation of individual beneficial microorganisms results in low colonization rates and limited functional expression[11,12]. Native microorganisms, for example, are known to be especially good in colonizing their soils and supporting function, especially under poor soils[13]. However, how to unravel the full potential to support food and plant-based industries remains poorly understood.

Increased research has focused on the enhancement of host growth and health function through SynComs with low complexity, high controllability, and high repeatability characteristics[11,14]. SynComs directly promote growth through beneficial functions, or amplify rhizosphere community functions of specific microbial groups by driving assembly of resident microbial communities[15]. However, how to select the members of the SynComs, what functional properties do they have and their location in the community are particularly important for the effective functioning of the SynComs. In fact, losing sight of the impact of proper ecological niches of functional microorganism and their

[1]State Key Laboratory of Tree Genetics and Breeding, Nanjing Forestry University, Nanjing 210037, China. [2]Key Laboratory of Soil Environment and Pollution Remediation, Institute of Soil Science, Chinese Academy of Sciences, Nanjing 210008, China. [3]Yongzhou Company of Hunan Tobacco Company, Yongzhou 425000, China. [4]Hunan Province Company of China Tobacco Corporation, Changsha 410004, China. [5]Laboratorio de Biodiversidad y Funcionamiento Ecosistémico, Instituto de Recursos Naturales y Agrobiología de Sevilla (IRNAS), CSIC, Sevilla, Spain. [6]These authors contributed equally: Yanyan Zhou, Donghui Liu. ✉e-mail: 199166853@qq.com; xgli@njfu.edu.cn

centrality in the interaction network may have adverse effects[16]. For example, the removal of *Enterobacter cloacae*, a keystone species on the roots of corn seedlings, led to the complete disappearance of the community[17]. The rhizoplane microbiome directly touches the roots and responds to the selection of the rhizoplane-root niche[18]. Moreover, the rhizoplane enriches a more specialized community, controlling the entry of microorganisms relevant to root system activity[19]. Therefore, it is necessary to focus on the rhizoplane niche to understand the laws of assembly and interaction of microbial communities from soil to rhizoplane, and utilize beneficial plant-microbial interactions to support plant growth.

Here, we posit that native core microbiomes associated with plant rhizoplane may hold the solution to harness the full potential of soil microbiomes to support plant growth. Native core taxa are expected to rapidly colonize and largely survive in their soils[20]. Moreover, core taxa solve one of the major issues of current SymComs, the capacity to support stable communities capable to survive in the soil for long time periods[21]. Low microbial survival rates and cost per application limit the contribution of soil microbiomes to support plant health and productivity[22,23]. Therefore, it is of great economic and environmental significance to search for low-cost, pollution-free, and sustainable new carrier materials and construct efficient and stable composite microbial fertilizer. Here, we seek to create a diverse and functionally stable community, based on core taxa, to promote plant growth by restoring microbial diversity, thereby providing beneficial services for plant growth.

To address this knowledge gap, we use tobacco (*Nicotiana tabacum* L.), an important plant-based industry of the planet, as our model system[24]. We adopted molecular statistics, culture isolation, and effect verification to obtain a SynComs SC2 with stable growth-promoting effects. SC2 increased the plant biomass by 76–91% in non-sterile environments. Biomass increase is related to the growth-promoting characteristics, pair compatibility, outstanding niche width, rhizosphere colonization of native core microorganisms, and improved growth-promoting function of the rhizosphere. Our results suggest that SynComs based on the native core microbiome of rhizoplanes can positively contribute to crop growth and further guide the improvement of crop yield in sustainable agriculture.

Results

Bacterial diversity and community assembly from soil to rhizoplane

To characterize the changes in microbial assembly processes of four soil types, we analyzed the 16 S sequencing data from three root-associated niches (Fig. 1a). After filtering, 2,963,984 high-quality reads were clustered into 162,876 ASVs based on the DADA2 clustering method. The Shannon and Chao1 indices showed a continuous decreasing trend from soil to rhizoplane, and significantly decreased by 37–76% in rhizoplane ($P < 0.001$, Fig. 2a). Even though different soils contain different microbial communities, there was no difference in their α-diversity at the rhizoplane, which indicates that plant rhizoplane can select a robust set of microbiota even across different soil types (Supplementary Fig. 1). The PERMANOVA and NMDS sequencing results showed that all samples differentiated primarily along the first axis of NMDS, indicating that the niche strongly influenced the microbial communities of all samples (Fig. 2b). In addition, the influence of soil type gradually decreased from bulk soil to rhizoplane (Supplementary Table 1). These results indicate that the specific recruitment of bacterial taxa on tobacco rhizoplane is robust despite the influence of different soil types.

We then investigated bacterial community composition from soil to rhizoplane, especially the bacterial microbial community in the rhizoplane. The bacterial communities of bulk soil and rhizosphere were mainly composed of Proteobacteria and Actinobacteria, which accounted for 17.3–52.0% of the total relative abundance depending on the soil type. The relative abundance of Proteobacteria and Firmicutes in the rhizoplane were significantly greater as compared to bulk soil and rhizosphere, and they dominated the rhizoplane bacterial community ($P < 0.05$, Supplementary Fig. 2).

Next, we determined the ASVs enrichment in plant rhizoplane in each soil type. The difference analysis indicated that 9.6–20.1% (230–319) of ASVs were significantly enriched in four different soil types ($P < 0.05$, Fig. 2c). Of these, 144 rhizoplane-enriched ASVs overlapped in at least three soils ($P < 0.05$, Fig. 2d). In addition, soil 4 has the most specifically enriched ASVs (108), while soil 2 has the most depleted ASVs (1378) (Fig. 2c, d). The overlapping ASVs were preferentially from *Bacillus*, *Pseudomonas*, *Paenibacillus*, and *Pseudoxanthomonas* (Fig. 2e). These results indicate that plants grown in different soils have a unique but overlapping core microbiome membership on the rhizoplane.

Acquisition of plant rhizoplane core ASVs

To further characterize the effects of plant selection on the bacterial microbiome, we assessed the symbiosis patterns of bacterial communities from soil to rhizoplane (Fig. 1a). In order to exclude the influence of low abundance microorganisms, ASVs presented in all soil types and whose relative abundances add up to >0.01% in all samples were retained. Therefore, 1103 ASVs shared across all soil type were selected (Supplementary Fig. 3a). Notably, these taxa accounted for 18.0% of ASV number and 64.6% of the total relative abundance in the total rhizoplane (Supplementary Fig. 3b). In the soil continuum from bulk soil to rhizoplane, the network complexity decreased significantly. The complexity of the bacterial network in bulk soil was the highest (average 51.90 degrees), and in rhizoplane was the lowest (average 18.31 degrees) (Supplementary Fig. 4). Notably, the number of hub-nodes significantly reduced from the bulk soil to the rhizosphere to the rhizoplane (Supplementary Fig. 4). The classification network of bulk soil and rhizosphere was similar, with most nodes representing Actinobacteria (29.8–34.2%) and Proteobacteria (29.1–35.7%). However, the classification network of the rhizoplane was preferentially composed of Proteobacteria (64.4%) and Firmicutes (25.6%) (Supplementary Fig. 4a). Compared to bulk soil, 93.3% of ASVs (168 out of 180 ASVs) were significantly enriched at rhizoplane (Supplementary Fig. 4b). Depleted index (DI) and difference index (DSI) were used to evaluate the filtering and selection of taxa from bulk soil, rhizosphere to rhizoplane. DI value decreased from bulk soil to rhizoplane, indicating that the rhizoplane selectively recruits bacterial taxa from bulk soil and rhizosphere (Supplementary Fig. 4c). Together, the results indicate that despite the differences in soil types, plant rhizoplane harbors similar bacteria that may have important functions for plant growth.

Combined with the results of network and difference analysis, 96 shared core ASVs enriched in tobacco rhizoplane (Fig. 3a). To obtain these ASVs, we first isolated and purified 101 strains in the plant rhizoplane. These bacteria preferentially belong to *Bacillus*, *Pseudomonas*, *Microbacterium*, *Dyadobacter*, and *Chryseobacterium* (Fig. 3b). To determine the consistency of the core ASV and isolates, the sequences of the two were compared in pairs. Based on 99% sequence similarity, 44 core ASVs were obtained. These matched ASVs preferentially belonged to *Bacillus* and *Pseudomonas*, and significantly enriched at the rhizoplane (Fig. 3b). Considering the taxonomic diversity of the candidate strains, we selected 22 matched isolates (native core microorganisms) and six non-matched isolates (native non-core microorganisms) of different species (Fig. 3b). In addition, YC14 and YC20 (non-native microorganisms) were derived from resource library of strains with excellent growth-promoting ability in the laboratory. In summary, 30 strains were selected, belonging to 30 species and 18 genera.

Growth-promoting effect of candidate strains on plant

After scaled screening microorganisms colonized in tobacco rhizoplane, a total collection of 30 strains belonging to different species was

https://doi.org/10.1038/s41467-024-50685-3

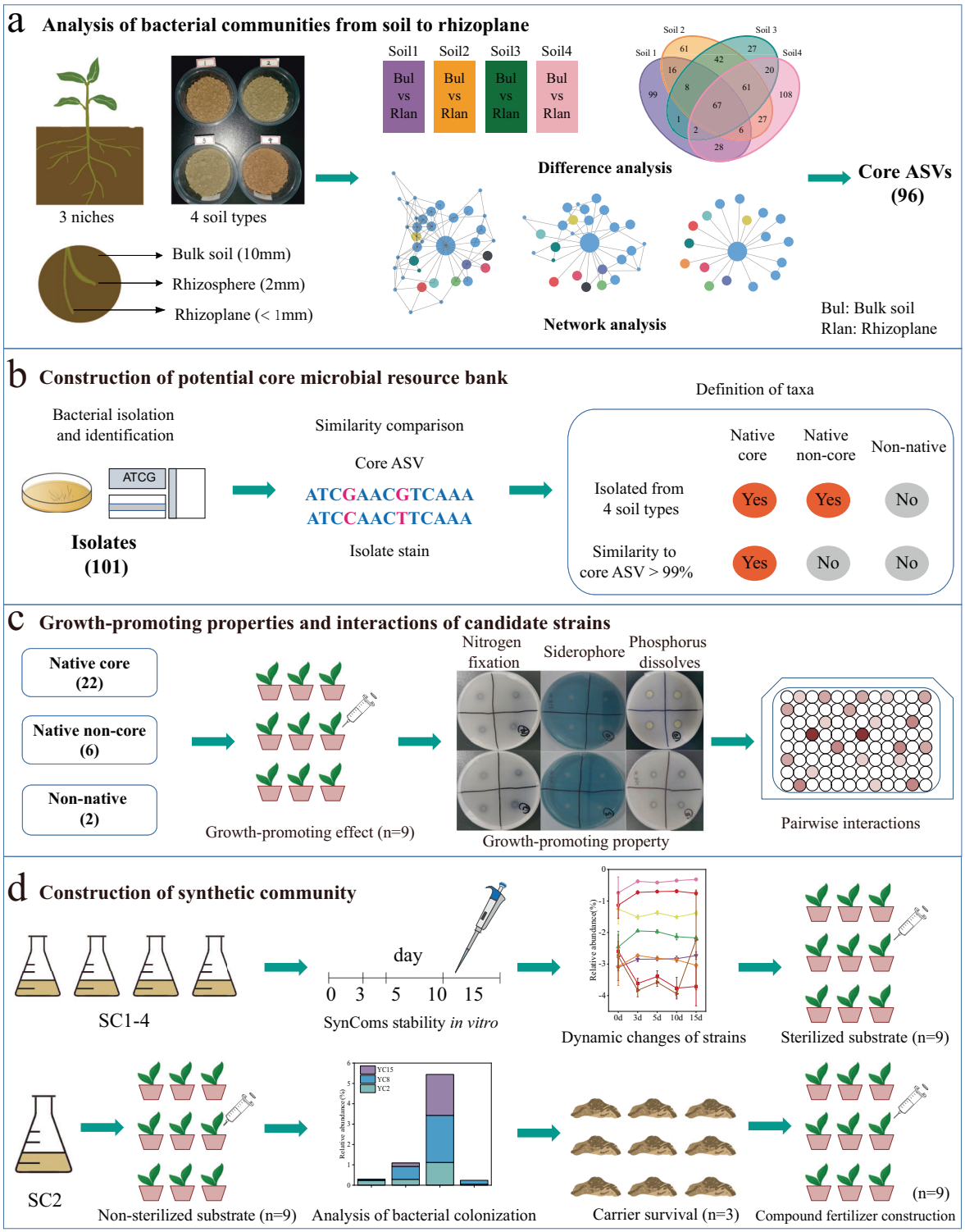

Fig. 1 | An overview of the experimental workflow for this study. a Sampling and analysis strategy of this study. **b** Construction of potential core microbial resource bank. **c** Growth-promoting properties and interactions of candidate strains. **d** Screening SynComs based on in vivo and in vitro interaction, and construction of composite fertilizers.

used to study their growth-promoting potential on tobacco (Fig. 1c). Compared with uninoculated plants, ten strains showed growth-promoting effects on tobacco, nevertheless, the remaining strains did not show significant promotion on shoot and root growth (Fig. 4a and Supplementary Fig. 5). Interestingly, with the exception of YC14 and YC20, all the growing-promoting strains matched the core ASVs. The strains, YC2, YC4, YC5, YC8, YC10, YC12, YC15, YC19, and YC20 inoculation significantly increased tobacco net biomass by 8–46% ($P < 0.01$, Fig. 4a and Supplementary Fig. 6). Among them, inoculation with YC2 and YC8 significantly increased shoot and root dry weight by 41% and 70%, respectively. In addition, ten strains also significantly contributed to the growth of total fresh weight of tobacco by

https://doi.org/10.1038/s41467-024-50685-3

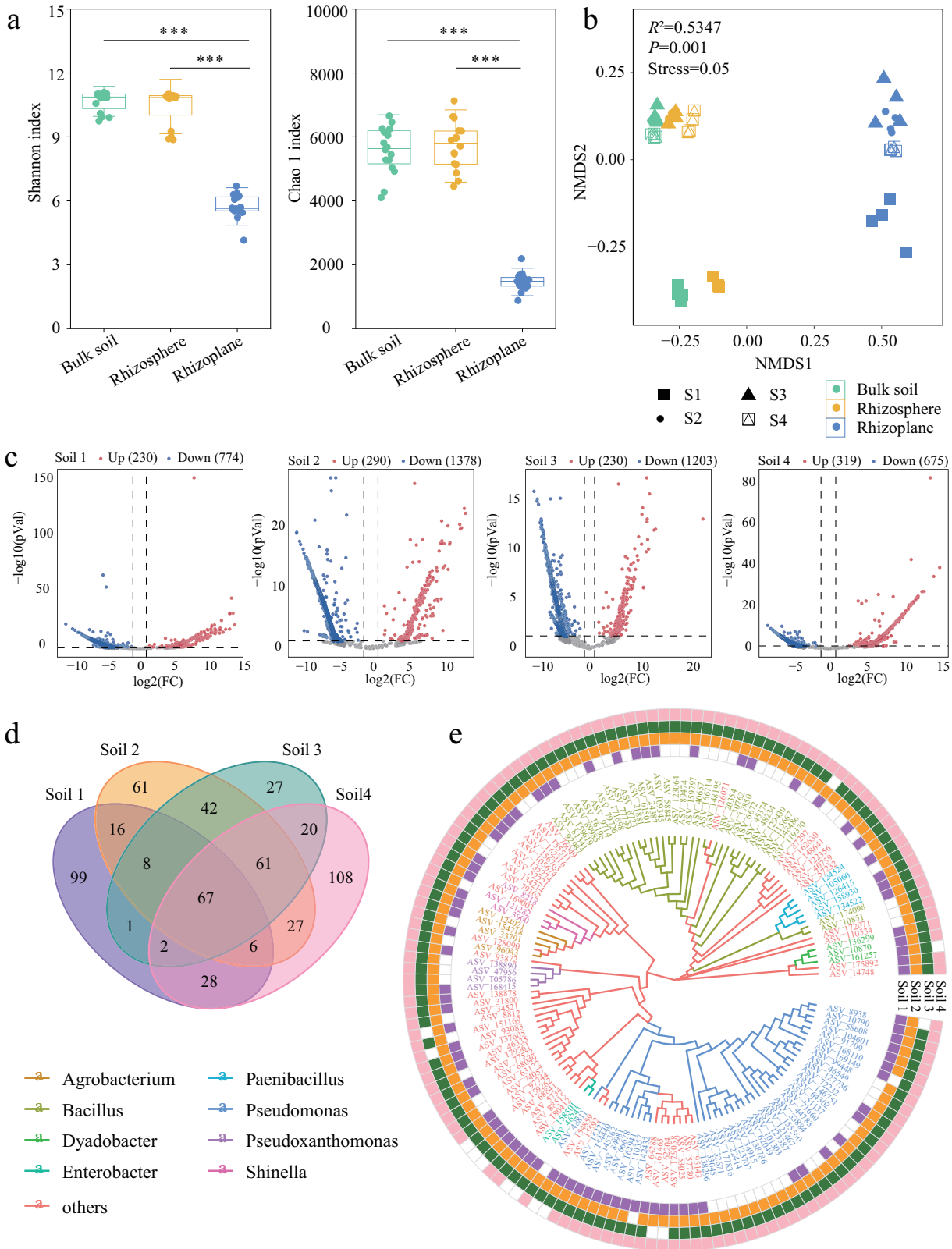

Fig. 2 | Bacterial diversity and community assembly from soil to rhizoplane. **a** Shannon and Chao1 index of the bacterial community from soil to rhizoplane. The significance of the difference was determined by a one-way ANOVA test ($n = 16$, $P < 0.001$). Horizontal bars within boxes represent the median. The tops and bottoms of boxes represent the 75th and 25th quartiles, respectively. The upper and lower whiskers represent SD. **b** NMDS analysis grouped by three compartment niches based on Bray-Curtis distance matrices of bacterial communities ($P < 0.001$, P value was calculated by one-way PERMANOVA). **C** Significantly enriched ASVs in the rhizoplane of each soil compared with bulk soil (DESeq2, $P < 0.05$, FDR adjustment). FC, fold change. **d** Venn diagram of significant enrichment of ASV in the rhizoplane of four soils. **e** Phylogenetic trees of enriched ASVs in at least three soils.

https://doi.org/10.1038/s41467-024-50685-3

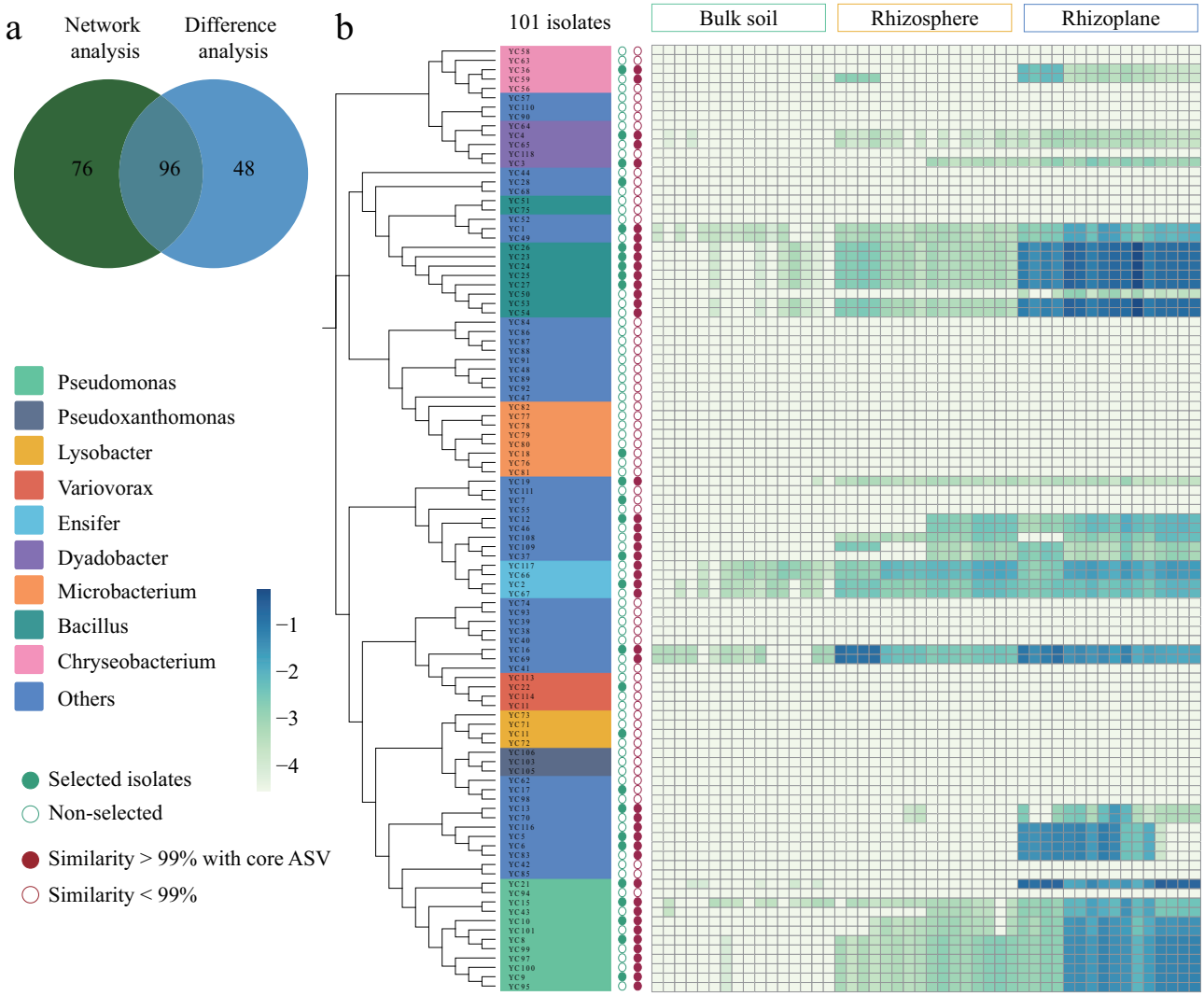

Fig. 3 | Acquisition of tobacco rhizoplane core ASVs. a Venn of rhizoplane enrichment ASVs in difference and network analysis. **b** The phylogenetic tree is constructed by isolated strains. Heatmap shows the relative abundance of core ASVs matched with isolated strains (sequence similarity >99%) from soil to rhizoplane.

promoting shoot and/or root fresh weight ($P < 0.01$, Supplementary Fig. 6). Consequently, we selected 10 strains of YC2, YC4, YCS, YC8, YC10, YC12, YC14, YC15, YC19, and YC20 which significantly promoted growth of tobacco to investigate their growth-promoting properties and colonizing ability.

Colonization experiments of a single strain in rhizoplane revealed that all growth-promoting strains were able to colonize on the rhizoplane of sterile seedling, and colonization rates began to stabilize after 3 weeks of inoculation (Supplementary Fig. 7). Among them, the number of native core microorganisms YC15 and YC8 in the tobacco rhizoplane increased by 10–15 times, which was significantly higher than other strains. One month after inoculation, the number of native non-core and non-native microorganisms on the tobacco rhizoplane increased less than fivefold (Supplementary Fig. 7). Subsequently, we investigated the capacity of IAA production, nitrogen fixation, solubilized phosphorus, and siderophore production of ten strains (Fig. 4a). Results indicated IAA content produced by seven strains ranged from 4.08 to 24.6 mg/L, among which YC10 produced the highest content of IAA, followed by YC8. Six strains grew on a nitrogen-free medium, but only the D/d ratio of YC5 was greater than 2, indicating its strong nitrogen fixation ability. In addition, YC5, YC8, YC10, and YC15 have the ability to solubilize phosphorus and produce siderophore (Fig. 4a).

Construction of SynComs and dynamics of in vivo interaction

In order to maximize the beneficial outcome of the growth-promoting bacteria and exclude the inhibitory effect of metabolites of one strain on the growth of others, we constructed SynComs based on the non-antagonism between pairwise interactions (Fig. 1c). First, pairwise interaction experiments indicated that most strains could coexist with each other and showed positive interaction. However, there were negative interactions between the two pairs of strains, namely YC19 and YC20, YC4 and YC12. Four SynComs were therefore constructed after excluding two antagonistic interactions (Fig. 4b).

Secondly, to determine the resource complementarity and survival dynamics of strains in each SynCom, we continuously tracked the survival status of the SynComs in medium five times in a row for a total of 15 days (Fig. 1d). Results revealed that relative abundance of strains changed greatly within 3 days of inoculation and then tended to be stable. Compared with other strains, the relative abundance of YC15, YC20, and YC5 remained stable at a high level (Fig. 4c). However, the relative abundance of YC2, YC4, YC12, and YC14 stabilized after significantly decreasing within 3 days of inoculation. Further analysis of the stability and niche breadth index of the SynComs showed that the AVD index of SC2 and SC4 was significantly lower than that of SC3 ($P < 0.01$, Fig. 4d). Niche width showed the opposite trend, and the niche width index of SC2 and SC4 was significantly higher than that of

https://doi.org/10.1038/s41467-024-50685-3

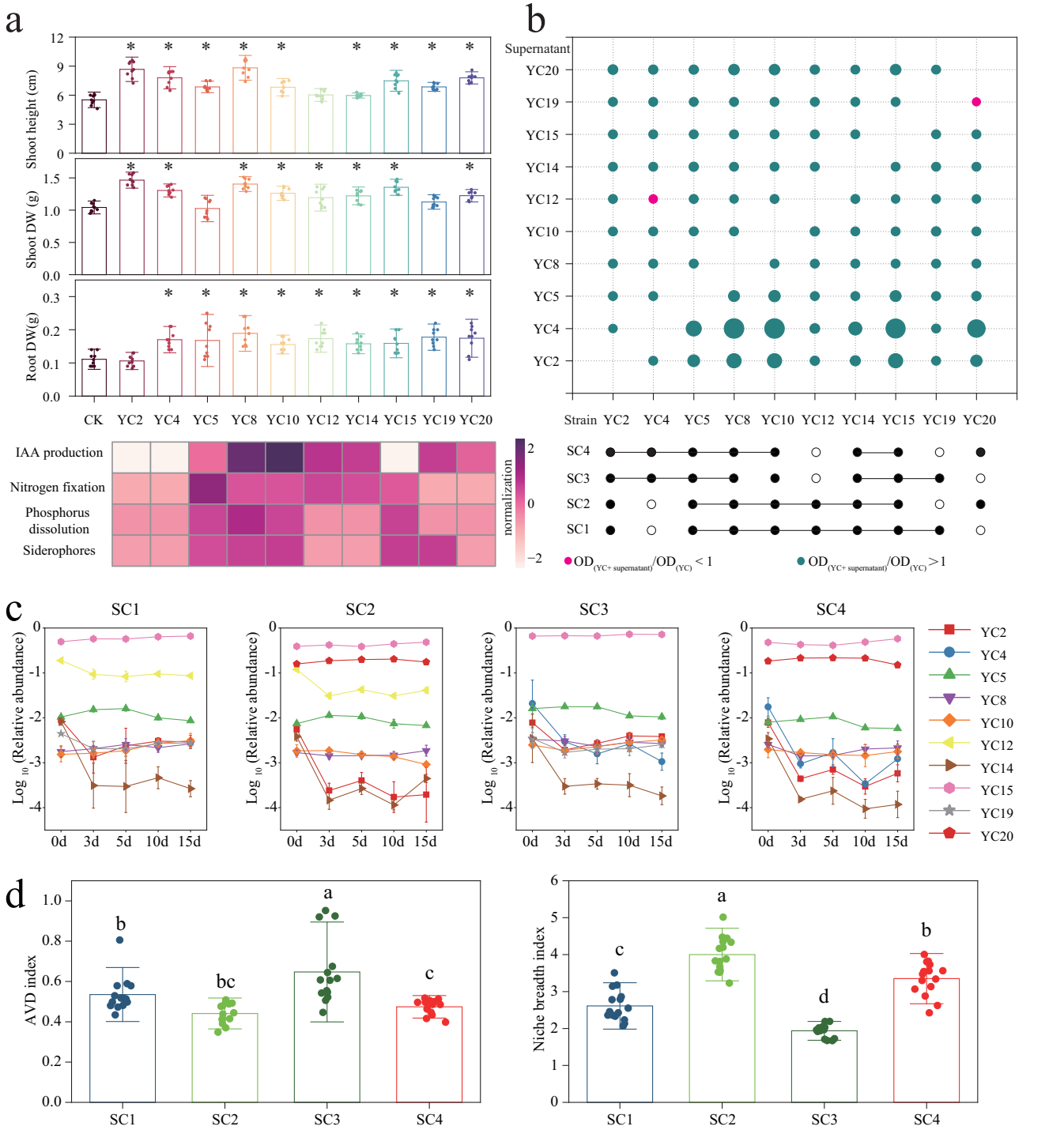

Fig. 4 | Screening of growth-promoting strains and construction of SynComs. **a** Evaluation of growth-promoting effect and properties of ten strains on tobacco. The asterisk on the bar chart means significantly higher than the control ($n = 9$, $P < 0.01$, one-way ANOVA test). **b** Construction of SynComs and pair interaction of growth-promoting bacteria. The size of the circle represents $OD_{(YC+\ supernatant)}/OD_{(YC)}$, and the growth-promoting effect of the supernatant on the other bacteria becomes stronger with the increase of the circle. **c** Survival status of the SynComs in the medium during cultivation of 15 days ($n = 3$). **d** Determination of SynComs stability in vitro and niche breadth index ($n = 15$, $P < 0.01$, one-way ANOVA test). AVD, average variation degree. Different letters on the boxplot indicate significant differences between treatments. Each bar represents the mean ± SD.

SC1 and SC3 ($P < 0.01$, Fig. 4d). Thus, SC2 had the highest community stability while SC3 had the lowest community stability.

Next, we conducted microbial interaction experiments in vivo to test the growth-promoting ability of the SynCom itself (Fig. 1d). SC2 inoculation significantly increased the shoot height, dry weight, and root fresh weight of tobacco compared with control and other SynComs treatments ($P < 0.01$, Supplementary Fig. 8). Shoot and total dry weight in SC2-treated plants were 52% and 83%, greater than the uninoculated plants ($P < 0.01$). However, SC2 inoculation did not significantly increase the shoot and total fresh weight of tobacco ($P > 0.05$, Supplementary Fig. 8). In conclusion, SC2, which significantly increased the net biomass of

https://doi.org/10.1038/s41467-024-50685-3

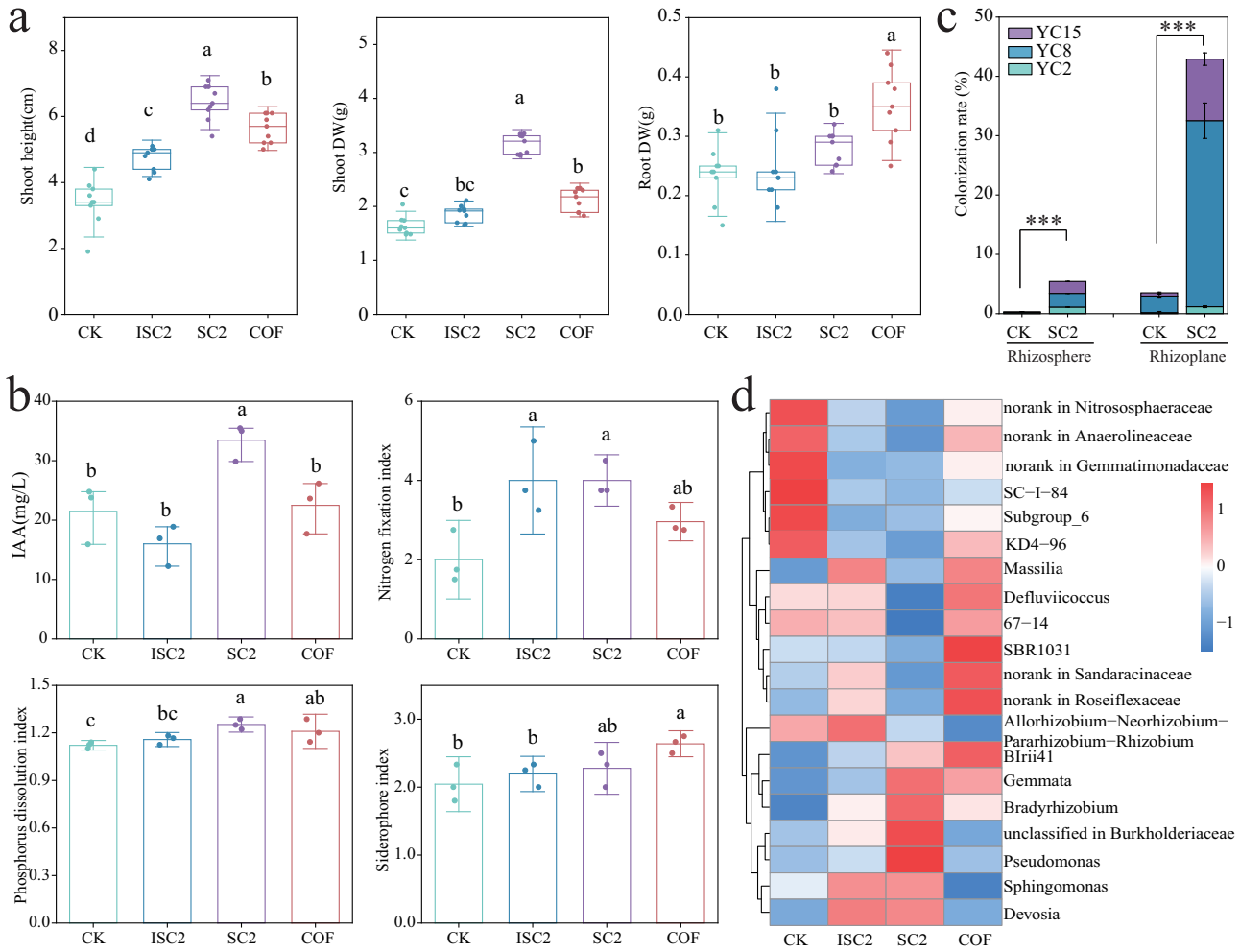

Fig. 5 | Effect verification and colonization analysis of SynComs in non-sterile environment. a Growth-promoting effect of different treatments on tobacco ($n = 9$, $P < 0.01$, one-way ANOVA test). Horizontal bars within boxes represent the median. The tops and bottoms of boxes represent the 75th and 25th quartiles, respectively. The upper and lower whiskers represent the SD. **b** Growth-promoting properties of rhizosphere microorganisms under different treatments ($n = 3$, $P < 0.05$, one-way ANOVA test). **c** Colonization ability of each strain of SC2 in rhizosphere and rhizoplane. Each bar represents the mean ± SD. **d** Heatmaps of the top 20 genera in relative abundance under different treatments. Different letters on the boxplot indicate significant differences between treatments. DW, dry weight. ISC2, inoculation of inactivated SC2; SC2, SC2 inoculation; COF, commercial organic fertilizer containing *Bacillus subtilis*; CK, without adding microorganisms as a control.

tobacco, was selected to study its stability in a non-sterile environment.

SC2-mediated phenotypic transfer to non-sterile environment

To study whether SC2-related phenotypes transfer to non-sterile soil conditions and whether SC2 drives the growth-promoting function of resident microbial communities, we conducted a 45-day pots experiment and measured the effects of SC2 inoculation on plant growth phenotypes (Fig. 1d). Compared with the control, inoculation of microorganisms (SC2 / *Bacillus subtilis*) promoted above and below ground biomass ($P < 0.01$). In addition, SC2 inoculation increased the aboveground biomass by 76%-91%, significantly higher than that of commercial bio-organic fertilizer treatment ($P < 0.01$, Fig. 5a and Supplementary Fig. 9). Different from promotion of commercial bio-organic fertilizer on plant root, SC2 inoculation had evident effect on prompting growth of tobacco above part ($P < 0.01$, Fig. 5a). However, inoculation with inactivated SC2 attenuated the growth-promoting effect on tobacco.

Thus, we focused on the growth-promoting ability of tobacco quality upon application of SC2. Indeed, the inoculated SC2 significantly increased the soluble protein and total nitrogen content of leaves ($P < 0.01$), but had no effect on the soluble sugar, reducing sugar, and total potassium content ($P > 0.05$, Supplementary Fig. 10). Especially, the ability of nitrogen fixation, IAA production, and dissolved phosphorus were significantly improved in tobacco rhizosphere, with approximately doubled increase ($P < 0.05$, Fig. 5b). However, the inoculated SC2 did not significantly enhanced activity of physiological enzymes (Supplementary Fig. 10).

To understand whether phenotypic transfer induced by microbial inoculation is associated with the colonization of members of SynComs, rhizosphere and rhizoplane soils were obtained and sequenced. The results revealed that YC2, YC8, and YC15 had more than 99% sequence similarity to specific ASVs and the relative abundance were significantly higher than control in rhizosphere and rhizoplane samples. It was noted that the sum of relative abundance of colonizing in the rhizoplane was even greater than 40%, which was significantly higher than in the rhizosphere ($P < 0.001$, Fig. 5c). In addition, the colonization rate of SC2 in the rhizosphere decreased significantly after the strains were inactivated ($P < 0.001$, Supplementary Fig. 11). These results revealed that YC2, YC8 and YC15 dominantly colonized on the tobacco rhizoplane. However, other strains were at a disadvantage in colonization in non-sterile environments. In addition,

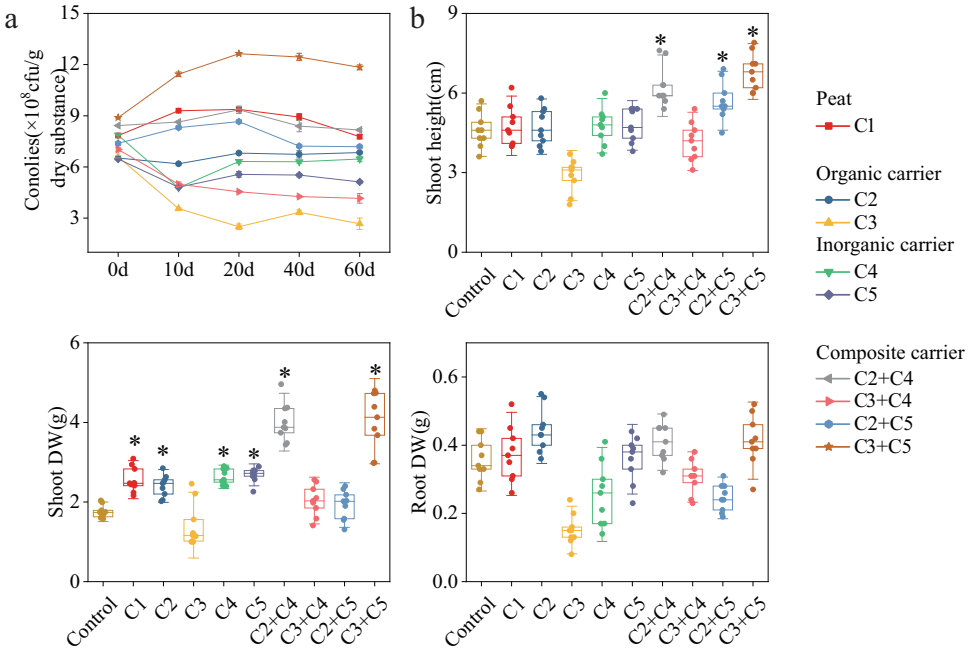

Fig. 6 | Construction and effect verification of microbial fertilizer. a The survival of SC2 in different carriers ($n = 3$). Each bar represents the mean ± SD. **b** Effect of constructed microbial fertilizer on tobacco growth ($n = 9$, $P < 0.001$, one-way ANOVA test). The asterisk on the bar chart means significantly higher than the control. DW, dry weight. C1, peat; C2, cow manure organic fertilizer; C3, rapeseed cake fertilizer; C4, diatomaceous earth; C5, rice husk carbon; C2 + C4, cow manure organic fertilizer + diatomaceous earth (organic fertilizer: diatomaceous earth = 1:1); C3 + C4, rapeseed cake fertilizer + diatomaceous earth; C2 + C5, cow manure organic fertilizer + rice husk carbon; C3 + C5, rapeseed cake fertilizer + rice husk carbon. Horizontal bars within boxes represent the median. The tops and bottoms of boxes represent the 75th and 25th quartiles, respectively. The upper and lower whiskers represent SD.

compared with other treatments, SC2 inoculation also significantly increased the relative abundance of *Gemmata*, *Bradyrhizobium*, *Pseudomonas*, and *Unclassified in Burkholderiaceae* in the rhizosphere ($P < 0.05$, Fig. 5d).

Compound microbial fertilizer stably promotes plant growth

Inoculation of carriers with plant beneficial bacteria could provide an approach to maintain the survival of inoculants after their application into fields. Therefore, we measured the survival of SC2 in organic, inorganic, and composite carriers. For different carriers, SC2 reached stable configuration at 10 d (Fig. 6). Interestingly, the composite carrier composed of rapeseed cake fertilizer and rice husk carbon was the most favorable for SC2 survival, and was the only carrier with higher survival rate than peat ($P < 0.01$). However, the survival rate of SC2 was the lowest in rapeseed cake fertilizer. In addition, except for the composite carriers composed of rapeseed cake fertilizer and diatomaceous earth, other composite carriers were more conducive to SC2 survival than single organic or inorganic carriers (Fig. 6).

Next, pot experiments were conducted to test the growth promotion effect of various microbial fertilizers in vivo. Consistent with the survival state of SC2 in carriers, the growth-promoting effect of composite microbial fertilizer composed of rapeseed cake fertilizer and rice husk carbon on tobacco was significantly higher than that of peat ($P < 0.01$), even though microbial fertilizer composed of rapeseed cake fertilizer alone was not beneficial to tobacco growth ($P > 0.05$, Fig. 6 and Supplementary Fig. 12). In addition, microbial fertilizer composed of cow manure and diatomaceous earth and rapeseed cake fertilizer and rice husk carbon significantly increased the aboveground and total biomass of tobacco by 103–129% ($P < 0.01$). Although fertilizers composed of peat, cow manure organic fertilizer, cow manure organic fertilizer and diatomaceous earth, rice husk carbon, and rapeseed cake fertilizer and rice husk carbon significantly increased the aboveground dry weight and total dry weight of tobacco, the growth promotion effect of fertilizer composed of composite carrier was higher than that of single carrier ($P < 0.05$, Fig. 6 and Supplementary Fig. 12).

Discussion

Land degradation and reduced yields caused by intensive management strategies hinder the sustainable development of agroecosystems[25]. Harnessing the beneficial properties of soil microorganisms is considered a promising way to sustainably increase plant production[26,27]. While many non-native beneficial microorganisms show promise under sterile conditions, it is difficult to transfer beneficial functions to the natural environment, wherein they can be outcompeted by native microorganisms facing difficulties during colonization[28]. In different soil environments and niches, we selected the native core and non-native microorganisms of tobacco rhizoplane to construct alternative SynComs. We found that although the SC2 (Synthetic community, based on six native core microorganisms and two non-native microorganisms) significantly promoted tobacco growth in a non-sterile environment, the native core microorganisms preferentially colonize the plant rhizosphere and rhizoplane. Our study provides solid evidence that, regardless of their functional potential, native core microorganisms have more opportunities to colonize and develop growth-promoting potential in host roots, compared with non-native microorganisms.

Direct screening of cultivable bacteria with specific functions from sites of interest to construct SynComs often results in poor application because the interaction of candidate strains in the native community is not directly considered[29,30]. One way to circumvent this problem is to design SynComs based on native core microbiomes, which are common across soils and provide critical support to plant communities[31]. Studies based on different hosts show that core taxa can overcome environmental dependence and widely adapt to host-related habitats[20,32]. Therefore, it is promising to identify the core microorganisms involved in the assembly of the host microbiome and manipulate them to produce applied benefits. The evaluation of maize

microbiome in different soil types, climatic zones, and genotypes showed that there was a highly conserved core taxa in maize xylem, and that SynComs based on the core taxa promoted plant growth through biological nitrogen fixation[31]. In our study, native non-core microorganisms failed to promote tobacco growth, and only native and non-native microorganisms were important supporters of plant growth. Native core microorganisms have greater potential to colonize tobacco rhizoplane and promote growth than non-native microorganisms.

Microorganisms in SynComs interact in many ways, they can inhibit each other by producing antibiotics, or support each other by cross-feeding[33]. However, the application of SynComs is largely hampered by losing sight of natural interactions among microbial members[34]. In this study, paired antagonism experiments retained bacteria that use each other's metabolic resources to promote mutual growth. In addition to this, SynComs as a whole faces niche competition and nutrient resources eaploitation[35,36]. In fact, in SynCom, it is not the members of the strong metabolic capacity but the members of the efficient use of metabolites that predominate[37]. Therefore, the rational and efficient use of resources, the reduction of resource overlap, and the expansion of the basic niche size of SynComs were the main determinants of success. Here, SC2 was selected for its superior niche width, AVD index, and significant growth-promoting ability.

Local microbial communities tend to be resilient in the face of new species, i.e. resistant to the input and restoring the original community structure[38,39]. Therefore, changing the microbiome types of native populations remains a major challenge for microbiome management. Native core microbiomes have more potential than non-native microbiomes because they have a home-field advantage and are, therefore, more likely to interact with resident microbiomes[13]. In fact, the non-native microorganism YC20 colonized disadvantageously in non-sterile environments, both rhizosphere and rhizoplane. However, the native core microorganisms YC2, YC8, and YC15 colonized strongly in non-sterile environments. These native core microbiomes act as pioneer symbionts to recruit potentially beneficial bacteria from the local pool of potential microbial symbionts, including *Gemmata*, *Bradyrhizobium*, and *Pseudomonas*[40,41]. In addition, the input of SC2 promoted the release of nutrient elements and the increase of auxin content. Therefore, SC2 promoted the growth of tobacco in the natural environment through the colonization of native core taxa and the improvement of rhizosphere growth-promoting function.

Taken together, our study shows that native core microorganisms have greater potential to increase plant yield than native non-core and non-native microorganisms. This potential can be attributed to the beneficial growth-promoting properties of the native core microorganisms, harmonious symbiosis within the community, and strong colonization capacity. However, the native non-core microorganisms do not have the ability to promote plant growth, and the non-native microorganisms lose their efficacy due to the non-home environment. This highlights the superiority of the native core microorganisms, and how they deliver the desired beneficial outcomes as a community. In summary, in the context of intensive farming and declining land quality, the native core microorganisms can be used as an alternative to optimize agro-ecosystem level production.

Methods

Experiment design and sampling strategy

Four types of soil were collected from representative fields (0–20 cm depth) in Yongzhou, Hunan province, with a planting history of rice and tobacco rotation (Fig. 1a). After removing the plant tissue and sifting through a 10 mm screen, the sampled soils were used for greenhouse experiment. Tobacco seeds were sterilized twice in 70% ethanol, rinsed in sterile distilled water, and then seeded on a nursery substrate. After 2 months of cultivation in a greenhouse, tobacco seedlings with matching sizes were selected, and each pot containing 2.5 kg of homogeneous soil (<10 mm) was planted with one seedling. Under the environmental conditions suitable for tobacco growth (28 ± 3 °C), 20 pots in each soil were placed in random blocks in the greenhouse.

Soil samples were collected 40 days after planting, and five tobacco roots were randomly mixed as a sample with a total of four replicates for each soil type. Gently shake the loose soils attached to roots as bulk soil samples. For the rhizosphere soil samples, the roots were rotated in 50 ml sterile phosphate buffered saline for 5 min, then the root was removed and centrifuged at 4000×*g* for 5 min. The roots were then put into a centrifuge tube containing phosphate buffer (25 ml). Ultrasound was performed at 120 W and 40 kHz (two times, 30 s). After the root removal, the remaining material was centrifuged at 4000×*g* for 10 min, and the precipitation was used as the rhizoplane soil. All samples were stored at −20 °C for DNA extraction.

Soil DNA extraction and amplicon sequencing

Soils (~500 mg) were weighted to extract total DNA using a FastDNA®SPIN Kit (MP Biomedicals, Solon, USA). The barcoded primers 341 F (5′-CCTAYGGGRBGCASCAG-3′)/806 R (5′- GGACTACNNGGGTATCTAAT-3′) were used to amplify the bacterial 16 S rRNA (V3–V4 region). The bacterial 16S rRNA gene were processed using USEARCH v10.0[42] and QIIME2[43]. Low-quality reads were discarded and paired sequences were merged. Amplicon sequence variant (ASV) was generated using the DADA2 pipeline and classified using the Silva database (v13.2). The sequence of all samples was flattened to the uniform data volume for subsequent analysis.

Isolation and identification of cultivable rhizoplane bacteria

Tobacco rhizoplane soils were suspended in PBS buffer, and then diluted to different concentrations (10^{-1}–10^{-7}) and plated on TSA agar (Soya peptone: 5 g, NaCl: 5 g, Casein peptone: 15 g, Agar: 15 g, Water: 1000 ml). After 3–7 days of culture, bacterial colonies were purified according to the morphology of the colonies. The 16S rRNA region of the obtained pure culture was amplified using 27 F (5′-AGAGTTTGATCCTGGCTC-3′) and 1492 R (5′-CGGCTACCTTGTTACGACTT-3′). The quality of amplified sequences was detected by agarose gel electrophoresis and sequenced in Sangon Biotech (Shanghai) Co., Ltd, China. In order to evaluate the consistency of isolated strains and core ASVs, the similarity between isolated strains and core ASVs was compared in pairs using Multiple Alignment using Fast Fourier Transform (MAFFT, https://www.ebi.ac.uk/jdispatcher/msa/mafft). When the similarity between isolated strain and core ASV is greater than 99%, they are believed to be the same strain (Fig. 1b).

Screening of tobacco growth-promoting bacteria

To maximize the diversity of candidate growth-promoting bacteria, 30 strains with different phylogeny at species level were selected. Among them, 22 strains were defined as native core microorganisms isolated from the tobacco rhizoplane with greater than 99% similarity to the core ASV. Six strains were defined as native non-core microorganisms isolated from the tobacco rhizoplane with less than 99% similarity to the core ASV. In addition, YC14 and YC20 are strains preserved in the laboratory for their excellent growth-promoting ability. In this study, they do not match any core ASVs and, therefore, are defined as non-native microorganisms. These bacteria covered 18 genera and 30 species. Bacterial strains were cultured in tryptic soy broth medium (TSB, 1.5 g/L tryptone, 0.5 g/L soytone, and 0.5 g/L sodium chloride) at 28 °C for 48 h. Bacterial cells were centrifuged, and resuspended in appropriate sterile water to a final density of 10^8 cells/mL as bacterial suspension. Tobacco seedlings and soil samples were obtained from the tobacco institute in Yongzhou, Hunan Province, China (26°42′N, 111°70′E). Tobacco seedlings with uniform growth were selected to plant in pots containing sterile soil and vermiculite (1:1, v/v). The experiment was conducted in a randomized block design

with 279 tobacco (ca. of nine replicates per treatment, 31 treatments). A volume of 10 mL of bacterial suspension was inoculated at days 10 and 30, and the control was inoculated with equal amounts of sterile water. Shoot height, shoot fresh and dry weight, and total fresh and dry weight were measured after 45 days of harvest.

Colonization of the rhizoplane by growth-promoting bacteria

In order to understand the colonization effect of ten grown-promoting strains on tobacco rhizoplane, we first constructed sterile tobacco seedlings. Tobacco seeds were sterilized with 75% ethanol (30 s) and 3% NaClO (15 min, three times), then placed in 1/2 strength Murashige and Skoog medium (MS) with 2% (wt/vol) sucrose and 0.8% (wt/vol) agar. Seven days after germination, the seedlings were transferred to 1/2 strength MS medium with three seedlings per medium. The culture was exposed to light at 22 °C for 16 h, darkness for 8 h, and continued for 7 days. Ten strains of growth-promoting bacteria were activated for fermentation at 30 °C and 170 r/min, and the concentration of bacteria solution was adjusted to OD_{600} = 0.1 with sterile water. Each plant was inoculated with 50 μl bacterial suspension. Each treatment had three replicates and each replicate had three parallels. From 14 to 28 days after inoculation, the bacteria were recovered once a week for a total of three times. Tobacco roots were rinsed with sterile water to remove floating bacteria. Then, the roots were placed in a PBS buffer for 5 min to extract the bacteria on the tobacco rhizoplane. After the roots were removed, the suspension was diluted and coated to determine the bacteria colonizing the rhizoplane.

Growth-promoting properties of rhizoplane bacteria

To understand the growth-promoting properties of these bacterial candidates, the ability of nitrogen fixation, phosphorus solubilization, siderophore, and IAA production of these strains were determined (Fig. 1c). Azotobacter, Pikovskaya, and CAS agar plates were added with two microliters of bacterial suspension and cultured at 28 °C for 5 days. Clear zones were observed on Azotobacter and Pikovskaya plates, and yellow-orange halo were observed on CAS plates, indicating that the strain had the ability of nitrogen fixation, phosphorus solubilization, and siderophore production, respectively[44]. The growth promotion ability of bacteria was quantitatively determined by the ratio (D/d) of clear zone or yellow-orange halo diameter (D) to colony diameter (d). Strains were cultivated in a TSB medium containing 5 mmol/L tryptophan. After culturing at 28 °C for 48 h, supernatant was obtained by centrifugation at 10,000 r/min for 5 min. One milliliter supernatant with the same amount of Salkawski chromogenic agent were placed in darkness for 30 min for the IAA chromogenic reaction. The color of the solution changes to pink as a positive reaction that the strains produce IAA. The yield of IAA of different strains was calculated by standard curve[45]. All treatments were tested in quadruple repetition with three parallels.

Determining pairwise interactions between rhizoplane growth-promoting bacteria

In order to understand the type of pair interaction between growth-promoting strains, i.e., convenience or antagonism, the growth of strains in the supernatant of other strains was compared with alone growth (Fig. 1c)[46]. In brief, after 48 h culture in TSA liquid media, monocultures of all strains were centrifuged to remove living cells. The strain was cultured at 30 °C for 12 h and adjusted to OD = 0.5 as overnight cultures. Subsequently, 180 μl sterile medium was supplemented with 20 μl supernatant of one strain and 2 μl overnight cultures of other strains. The strain supernatant was replaced by a sterile medium of equal quantity as control. All treatments were cultured at 30 °C for 24 h (170 rpm), and the optical density was measured at 600 nm. The type of paired interaction between the two species was determined by calculating the ratio of supernatant-treated bacterial concentration $OD_{(YC+\ supernatant)}$ with the single bacterial concentration $OD_{(YC)}$. We expected that the interaction would be facilitative if $OD_{(YC+\ supernatant)}/OD_{(YC)} > 1$ and antagonistic if $OD_{(YC+supernatant)}/OD_{(YC)} < 1$. All treatments were tested in triplicates.

Determination of stability of SynCom in vitro

Four SynComs (SC1–SC4) were initially assembled according to the principle of non-antagonism between pairwise interactions in SynComs (Fig. 1d). The ten strains were separately activated in TSA liquid medium for 48 h and the optical density was adjusted to 1 (600 nm). Equal volumes of each strain were pooled to generate community working stock, resulted in a total of four SynComs. Community working stock was inoculated into 50 ml of sterilized TSA liquid medium at 2% inoculum. The co-culture system without microorganisms was used as control (Control). For each SynCom, three 10 mL cultures were collected at 0, 3, 5, 10, and 15 d, and total no. 60 cultures were processed for amplicon sequencing. The 16S rRNA sequence of each strain was compared with the OTUs sequence in cultures, and the strain with a matching degree of more than 97% was retained. The relative abundance of the retained strains was dynamically examined to determine the survival status of the strains in the SynComs.

Determination of interaction effects of SynComs in vivo

We further investigated in vivo interactions of SynComs based on sterilized control experiments (Fig. 1d). For the suspension of SynComs, after mixing a single bacterial culture of equal volume (OD_{600} = 1), the final inoculation concentration of the mixture was adjusted to OD_{600} = 1. All treatments inoculate equal amounts of the mixture. Consistent with an assessment of the growth-promoting ability of individual bacteria, inoculation with sterile water was considered as the control. Five block groups were randomly designed with nine replicates per block group. The status of plant growth was measured after 45 days of harvest.

Evaluation of SC2 on tobacco growth in a non-sterilized environment

To investigate the stability of growth-promoting function of SC2 in non-sterile environment, we conducted a 45-d pots experiment using an unsterilized soil and vermiculite (1:1, v/v, Fig. 1d). There were four different treatments: ISC2, inoculation of inactivated SC2; SC2, SC2 inoculation; COF, commercial organic fertilizer containing *Bacillus subtilis*; CK, without adding fertilizer substrate as a control. Except for the control, the inoculated amounts of other treated bacteria were consistent. A randomized complete block design was employed to conduct the pot experiment with nine replicates. As described above, growth indicators and growth-promoting properties of the tobacco were measured after harvest. In addition, the fresh tobacco leaves were grouped into two parts. One portion was stored at −80 °C for the determination of soluble sugar, reducing sugar content, protein content, and defense enzyme activity, and another portion was decolorized for the determination of nicotine, total nitrogen, and total potassium. Tobacco rhizosphere (all treatment) and rhizoplane (only samples of control and SC2 treatment) soil was extracted for amplicon sequencing of bacterial communities. The 16S rRNA sequence of the strain matched with ASV and the relative abundance > 1% were the indicators of bacterial colonization.

Plant physiological and biochemical response to SC2 inoculation

Total soluble protein was determined using bovine serum albumin as a standard[47]. The content of soluble sugar was determined by a throne method, absorbance of the mixture was determined at 620 nm[48]. Reducing sugars were determined using the method adopted by Jan and Roel[49]. Superoxide dismutase (SOD) and peroxidase (POD) activities were determined according to the method of Kochs et al.[50] and Wang et al.[51], respectively. One unit of SOD and POD activity was

defined as an absorbance of 0.01 per minute in $OD560_{nm}$ and $OD470_{nm}$, respectively. Using the colorimetric method, tobacco leaves were dried and crushed for the determination of nicotine content[52].

Survival of SC2 in different carriers

The bacterial inoculants were prepared in following formulations: C1, peat; C2, cow manure organic fertilizer; C3, rapeseed cake fertilizer; C4, diatomaceous earth; C5, rice husk carbon; C2 + C4, cow manure organic fertilizer + diatomaceous earth (organic fertilizer: diatomaceous earth = 1:1, v:v); C3 + C4, rapeseed cake fertilizer + diatomaceous earth; C2 + C5, cow manure organic fertilizer + rice husk carbon; C3 + C5, rapeseed cake fertilizer + rice husk carbon. One hundred grams of sterile pure carriers and mixed carriers (equal amount of mixture) were added into the flask, and 5 ml SC2 was inoculated with each carrier. After 10, 20, 40, and 60 days of inoculation, the number of viable bacteria in different carrier fertilizers was determined by the dilution coating board method. Two-gram carrier fertilizers were added to a triangular flask containing 20 mL of sterile water. Carrier fertilizer was shaken 2 h as 10^{-1} bacterial suspension. Bacterial suspension continuously diluted to 10^{-6} was applied to the TSA medium. Colonies were counted after 2 d of incubation and three parallels were set for each treatment.

Effect of different microbial fertilizers on tobacco growth

Water conditioning is performed on all sterile carriers to ensure that the water content of the carriers remains consistent. SC2 suspensions were inoculated into carries in 5% proportion and cultured for 3 days after full mixing to prepare microbial fertilizer. Uniformly grown tobacco seedlings were planted in pots filled with substrates mixed 1:1 (v:v) with tobacco soil. Tobacco roots were sprinkled with 10 g of microbial fertilizer made from the above nine types of carriers, and tobaccos without fertilizer were used as control. Each microbial fertilizer was performed using a randomized complete block design with nine replicates. Plants were harvested at 30 d and tobacco related growth promotion indicators were measured.

Statistical analysis

All statistical analyses in this study were carried out in R v.3.6.3. Alpha diversity was calculated based on the rarefied ASVs table using the vegan package. The Bray-Curtis distance matrix was calculated and the β-diversity of the community was analyzed by non-metric multidimensional scaling (NMDS). Permutational multivariate analyses of variance (PERMANOVA) were used to examine the difference in community structure. The R package DESeq2 was used to compare differences in the relative abundance of ASVs. Only ASVs with $P < 0.05$ (FDR-adjusted) and $\log_2$ (fold change) >2 or <−2 were regarded as significantly difference.

The SparCC was used to assess the complexity of co-occurrence networks of different niches. To exclude the effect of low abundance ASVs in the network, the ASVs of the sum of relative abundance >0.01% and present in all soil types were retained. Nodes were retained based on statistical significance ($P < 0.05$) and robust correlation coefficients ($r > 0.6$ or $r<-0.6$). In addition, indexes (the number of edges and nodes, modularity and average degree, etc.) were used to characterize the topology of the co-occurrence network. The network was visualized in Gephi[53]. The ratio of depleted ASV to enriched ASV is used to represent the depletion index (DI). The ratio of the number of differential ASVs to the total number of ASVs is used to represent the dissimilarity index (DSI)[54].

The average variation degree (AVD) were calculated to examine microbial communities stability according to the method of ref. 55. A lower AVD value indicates higher microbiome stability. The "niche breadth index" was calculated using "spaa" R packeage[56]. One-way analysis of variance (ANOVA) was used to compare significant differences between control and different inoculation treatments.

Reporting summary

Further information on research design is available in the Nature Portfolio Reporting Summary linked to this article.

Data availability

The raw reads from Illumina sequencing described in this study have been deposited in the NCBI database under accession code PRJNA941096. Source data are available in 'figshare' with the identifier https://doi.org/10.6084/m9.figshare.26097025. Source data are provided with this paper.

Code availability

Codes used in this study are available in the Figshare database (https://doi.org/10.6084/m9.figshare.25751679).

References

1. Hartmann, M. & Six, J. Soil structure and microbiome functions in agroecosystems. *Nat. Rev. Earth Environ.* **4**, 4–18 (2023).
2. Jansson J. K., Mcclure R. & Egbert R. G. Soil microbiome engineering for sustainability in a changing environment. *Nat. Biotechnol*. **41**, 1716–1728 (2023).
3. Trivedi, P. et al. Plant-microbiome interactions: from community assembly to plant health. *Nat. Rev. Microbiol*. **18**, 607–621 (2020).
4. Edwards, J. et al. Structure, variation, and assembly of the root-associated microbiomes of rice. *Proc. Natl Acad. Sci. USA* **112**, E911–E920 (2015).
5. Guo, J. J. et al. Seed-borne, endospheric and rhizospheric core microbiota as predictors of plant functional traits across rice cultivars are dominated by deterministic processes. *N. Phytol*. **230**, 2047–2060 (2021).
6. Sun, X. L. et al. *Bacillus velezensis* stimulates resident rhizosphere *Pseudomonas stutzeri* for plant health through metabolic interactions. *ISME J*. **16**, 774–787 (2022).
7. Li, Z. F. et al. A simplified synthetic community rescues Astragalus mongholicus from root rot disease by activating plant-induced systemic resistance. *Microbiome* **9**, 217 (2021).
8. Qu, Q. et al. Rhizosphere microbiome assembly and its impact on plant growth. *J. Agric. Food Chem.* **68**, 5024–5038 (2020).
9. Saeed, Q. et al. Rhizosphere bacteria in plant growth promotion, biocontrol, and bioremediation of contaminated sites: a comprehensive review of effects and mechanisms. *Int. J. Mol. Sci*. **22**, 10529 (2021).
10. Singh, B. K. et al. Crop microbiome and sustainable agriculture. *Nat. Rev. Microbiol* **18**, 601–602 (2021).
11. Mawarda, P. C., Le Roux, X., Van Elsas, J. D. & Salles, J. F. Deliberate introduction of invisible invaders: a critical appraisal of the impact of microbial inoculants on soil microbial communities. *Soil Biol. Biochem*. **148**, 107874 (2020).
12. De, S. R., Adriana, A. & Passaglia, L. Plant growth-promoting bacteria as inoculants in agricultural soils. *Genet. Mol. Biol.* **38**, 401–419 (2015).
13. Jiang, M. T. et al. Home-based microbial solution to boost crop growth in low-fertility soil. *N. Phytol*. **239**, 752–765 (2023).
14. Berendsen et al. Disease-induced assemblage of a plant-beneficial bacterial consortium. *ISME J*. **12**, 1496–1507 (2018).
15. Hu, J. et al. Introduction of probiotic bacterial consortia promotes plant growth via impacts on the resident rhizosphere microbiome. *Proc. R. Soc. B Biol. Sci*. **288**, 20211396 (2021).
16. Haskett, T. L., Tkacz, A. & Poole, P. S. Engineering rhizobacteria for sustainable agriculture. *ISME J*. **15**, 949–964 (2021).
17. Niu, B., Paulson, J. N., Zheng, X. Q. & Kolter, R. Simplified and representative bacterial community of maize roots. *Proc. Natl Acad. Sci*. **114**, E2450–E2459 (2017).

18. Li, Y. Z. et al. Root exudation processes induce the utilization of microbial-derived components by rhizoplane microbiota under conservation agriculture. *Soil. Biol. Biochem*. **178**, 108956 (2023).
19. Zhang, Y. Z. et al. Huanglongbing impairs the rhizosphere-to-rhizoplane enrichment process of the citrus root-associated microbiome. *Microbiome* **5**, 97 (2017).
20. Toju, H. et al. Core microbiomes for sustainable agroecosystems. *Nat. Plants* **4**, 247–257 (2018).
21. Lemanceau, P., Blouin, M., Muller, D. & Moënne-Loccoz, Y. Let the core microbiota be functional. *Trends Plant Sci*. **22**, 583–595 (2017).
22. Sun, D. Q., Hale, L. & Crowley, D. Nutrient supplementation of pinewood biochar for use as a bacterial inoculum carrier. *Biol. Fertil. Soils* **52**, 515–522 (2016).
23. Herrmann, L. & Lesueur, D. Challenges of formulation and quality of biofertilizers for successful inoculation. *Appl. Microbiol. Biotechnol*. **97**, 8859–8873 (2013).
24. Li, J. X. et al. Multi-factor correlation analysis of the effect of root-promoting practices on tobacco rhizosphere microecology in growth stages. *Microbiol. Res*. **270**, 127349 (2023).
25. Coban, O., De Deyn, G. B. & Van Der Ploeg, M. Soil microbiota as game-changers in restoration of degraded lands. *Science* **375**, 990-+ (2022).
26. Hiruma, K. et al. Root endophyte Colletotrichum tofieldiae confers plant fitness benefits that are phosphate status dependent. *Cell* **165**, 464–474 (2016).
27. Liu, C. Y. et al. Root microbiota confers rice resistance to aluminium toxicity and phosphorus deficiency in acidic soils. *Nat. Food* **4**, 912–924 (2023).
28. Fukami, J., Nogueira, M. A., Araujo, R. S. & Hungria, M. Accessing inoculation methods of maize and wheat with Azospirillum brasilense. *AMB Express* **6**, 3 (2016).
29. Lin, Y. X. et al. The bacterial consortia promote plant growth and secondary metabolite accumulation in Astragalus mongholicus under drought stress. *BMC Plant Biol*. **22**, 475 (2022).
30. Lawson, C. E. et al. Common principles and best practices for engineering microbiomes. *Nat. Rev. Microbiol*. **17**, 725–741 (2019).
31. Zhang, L. Y. et al. A highly conserved core bacterial microbiota with nitrogen-fixation capacity inhabits the xylem sap in maize plants. *Nat. Commun*. **13**, 3361 (2022).
32. Hong, S. et al. Selection of rhizosphere communities of diverse rotation crops reveals unique core microbiome associated with reduced banana Fusarium wilt disease. *N. Phytol*. **238**, 2194–2209 (2023).
33. Culp, E. J. & Goodman, A. L. Cross-feeding in the gut microbiome: ecology and mechanisms. *Cell Host Microbe* **31**, 485–499 (2023).
34. Ratzke, C., Barrere, J. & Gore, J. Strength of species interactions determines biodiversity and stability in microbial communities. *Nat. Ecol. Evol*. **4**, 376 (2020).
35. Freilich, S. et al. Competitive and cooperative metabolic interactions in bacterial communities. *Nat. Commun*. **2**, 589 (2011).
36. Yang, T. J. et al. Resource availability modulates biodiversity-invasion relationships by altering competitive interactions-invasion relationships by altering competitive interactions. *Environ. Microbiol*. **19**, 2984–2991 (2017).
37. Mcclure, R. et al. Interaction networks are driven by community-responsive phenotypes in a chitin-degrading consortium of soil microbes. *Msystems* **7**, e0037222 (2022).
38. Moya, A. & Ferrer, M. Functional redundancy-induced stability of gut microbiota subjected to disturbance. *Trends Microbiol*. **24**, 402–413 (2016).
39. Schmitz, L. et al. Synthetic bacterial community derived from a desert rhizosphere confers salt stress resilience to tomato in the presence of a soil microbiome. *ISME J*. **16**, 1907–1920 (2022).
40. Da Silva, T. R. et al. Not just passengers, but co-pilots! Non-rhizobial nodule-associated bacteria promote cowpea growth and symbiosis with (brady)rhizobia. *J. Appl. Microbiol*. **134**, lxac013 (2022).
41. Tao, C. et al. Bio-organic fertilizers stimulate indigenous soil Pseudomonas populations to enhance plant disease suppression. *Microbiome* **8**, 137 (2020).
42. Rognes, T. et al. VSEARCH: a versatile open source tool for metagenomics. *Peerj*.**4**, e2584 (2016).
43. Bolyen, E. et al. Reproducible, interactive, scalable and extensible microbiome data science using QIIME 2. *Nat. Biotechnol*. **37**, 852–857 (2019).
44. Lynne, A. M., Haarmann, D. & Louden, B. C. Use of Blue Agar CAS assay for siderophore detection. *J. Microbiol. Biol. Edu*. **12**, 51–53 (2011).
45. Glickmann, E. & Dessaux, Y. A critical examination of the specificity of the salkowski reagent for indolic compounds produced by phytopathogenic bacteria. *Appl Environ. Microbiol*. **61**, 793–796 (1995).
46. Li, M. et al. Facilitation promotes invasions in plant-associated microbial communities. *Ecol. Lett*. **22**, 149–158 (2019).
47. Bradford, M. M. A rapid and sensitive method for the quantitation of microgram quantities of protein utilizing the principle of protein-dye binding. *Anal. Biochem*. **72**, 248–254 (1976).
48. Hansen, J. & Moller, I. Percolation of starch and soluble carbohydrates from plant tissue for quantitative determination with anthrone. *Anal. Biochem*. **68**, 87–94 (1975).
49. Jan, B. & Roel, M. An improved colorimetric method to quantify sugar content of plant tissue. *J. Exp. Bot*. **44**, 1627–1629 (1993).
50. Kochs, G. & Grisebach, H. Enzymic synthesis of isoflavones. *Eur. J. Biochem*. **155**, 311–318 (1986).
51. Wang, Y. S., Tian, S. P. & Xu, Y. Effects of high oxygen concentration on pro- and anti-oxidant enzymes in peach fruits during postharvest periods. *Food Chem*. **91**, 99–104 (2005).
52. Schmid, H. & Serrano, M. Untersuchungen über die Nikotinbildung des Tabaks. *Experientia* **4**, 311–312 (1948).
53. Bastian, M., Heymann, S. & Jacomy, M. Gephi: An Open Source Software for Exploring and Manipulating Networks. *International AAAI Conference on Weblogs and Social Media*. (2009).
54. Li, F. Q. et al. Host plant selectionimprints structure and assembly of fungal community along the soil-root continuum. *Msystems* **7**, e00361–22 (2022).
55. Xun, W. B. et al. Specialized metabolic functions of keystone taxa sustain soil microbiome stability. *Microbiome*. **9**, 35 (2021).
56. Zhang, J. et al. Distinct large-scale biogeographic patterns of fungal communities in bulk soil and soybean rhizosphere in China. *Sci. Total Environ*. **644**, 791 (2018).

Acknowledgements

This research was supported by the National Natural Science Foundation of China 32122056 (X.G.L.), the National Key Research and Development Program of China 2022YFD2201900 (X.G.L.), and the Science and Technology Projects of Hunan Company of China Tobacco Corporation 18-20Aa03 (Z.J.) and Hubei Company of China Tobacco Corporation 027Y2022-001 (Y.D.). M.D.-B. acknowledges support from TED2021-130908B-C41/AEI/10.13039/501100011033/Unión Europea NextGenerationEU/PRTR and from the Spanish Ministry of Science and Innovation for the I + D + i project PID2020-115813RA-I00 funded by MCIN/AEI/10.13039/501100011033.

Author contributions

Y.Z. and D.L. conducted data curation, methodology, and writing-original draft. XG.L. conceived the project, designed the experiments, and writing-original draft. F.L. implemented methodology. Y.D. and Y.L. reviewed the manuscript. Z.J., S.P., XH.L., and M.D.-B. edited the manuscript. All authors have discussed the results and read and approved the contents of the manuscript.

Competing interests
The authors declare no competing interests.

Additional information
Supplementary information The online version contains supplementary material available at https://doi.org/10.1038/s41467-024-50685-3.

Correspondence and requests for materials should be addressed to Shuguang Peng or Xiaogang Li.

Peer review information *Nature Communications* thanks the anonymous, reviewer(s) for their contribution to the peer review of this work. A peer review file is available.